ACS APPLIED MATERIALS & INTERFACES

Research Article

www.acsami.org

Mix and Match: Coassembly of Amphiphilic Dendrimers and Phospholipids Creates Robust, Modular, and Controllable Interfaces

Samuel S. Hinman,[†] Charles J. Ruiz,[‡] Yu Cao,[§] Meghann C. Ma,[‡] Jingjie Tang,[§] Erik Laurini,[∥] Paola Posocco,[∥] Suzanne Giorgio,[§] Sabrina Pricl,[∥] Ling Peng,*[,§] and Quan Cheng*[,†,‡]

[†]Environmental Toxicology and [‡]Department of Chemistry, University of California, Riverside, Riverside, California 92521, United States

[§]CNRS, Centre Interdisciplinaire de Nanoscience de Marseille (CINaM), Equipe Labellisée Ligue Contre le Cancer, Aix-Marseille University, 13288 Marseille, France

[∥]Molecular Simulation Engineering (MOSE) Laboratory, Department of Engineering and Architecture (DEA), Trieste University, 34127 Trieste, Italy

Supporting Information

ABSTRACT: Self-assembly of supramolecular structures has become an attractive means to create new biologically inspired materials and interfaces. We report the first robust hybrid bilayer systems readily coassembled from amphiphilic dendrimers and a naturally occurring phospholipid. Both concentration and generation of the dendrimers have direct impacts on the biophysical properties of the coassemblies. Raising the dendrimer concentration increases the hybrid bilayer stability, while changes in the generation and the concentration of the embedded dendrimers impact the fluidity of the coassembled systems. Multivalent dendrimer amine terminals allow for nondestructive *in situ* derivatization, providing a convenient approach to decorate and modulate the local environment of the hybrid bilayer. The coassembly of lipid/dendrimer interfaces offers a unique platform for the creation of hybrid systems with modular and precisely controllable behavior for further applications in sensing and drug delivery.

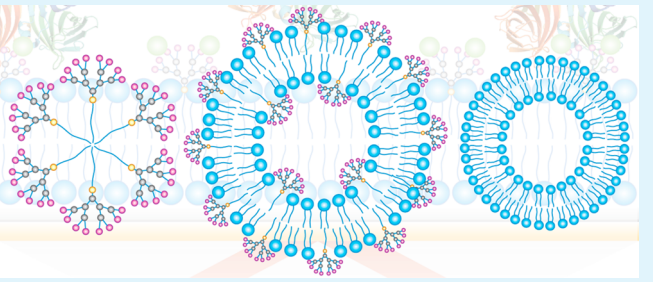

KEYWORDS: *amphiphilic dendrimers, dendrimer/lipid hybrid membrane, self-assembly, supramolecular coassembly, surface plasmon resonance*

INTRODUCTION

Self-assembly of supramolecular complexes derived from biological and synthetic components is an important strategy to establish novel materials and interfaces.[1−3] These complexes include many classes, such as those derived from proteins, nucleic acids, lipids, polymers, or metal nanoparticles, and the interactions between them have many implications for their assembly pathways and dynamic geometries. One promising application of these constructs is based on their ability to sense, detect and transport biologically interesting agents, particularly in regards to self-assembled lipid and polymer nanostructures for drug delivery.[4] Both lipids and polymers are capable of assembling with the therapeutic agent to be delivered, providing protection from biodegrading physiological environments while improving bioavailability in order to bring the therapeutic cargo to the target site intact.

One specific type of synthetic polymer known as dendrimers is particularly appealing for drug delivery by virtue of their well-defined structure with unique radial architecture, numerous terminal functionalities, and various interior cavities.[5−7] Polyamidoamine (PAMAM) dendrimers, originally developed by Tomalia as protein mimics with a large number of amide functionalities in the interior and primary amine terminals on the surface,[8,9] have been the most extensively studied for biomedical applications.[7] Recently, amphiphilic dendrimers, constructed from long hydrophobic alkyl chains and PAMAM dendrons, have emerged as newcomers in the drug delivery field. These amphiphilic dendrimers are able to capitalize on the delivery features of lipid and polymer vectors while minimizing adverse toxic effects.[10−12] They can assemble into supramolecular nanostructures and can be loaded with therapeutic cargos, either through hydrophobic encapsulation within the interior of a dendrimer nanomicelle[11] or via electrostatic interaction with the charged amine functionalities on the dendrimer surface.[12−14] While these assemblies have proved highly effective compared to traditional lipid or dendrimer vectors, interest is growing around the coassembly of synthetic compounds with naturally occurring phospholipids for the assembled constructs' potential to demonstrate both natural and tunable biophysical properties.[15−18] In this line, we

Received: September 12, 2016
Accepted: December 13, 2016
Published: December 13, 2016

DOI: 10.1021/acsami.6b11556
ACS Appl. Mater. Interfaces XXXX, XXX, XXX−XXX

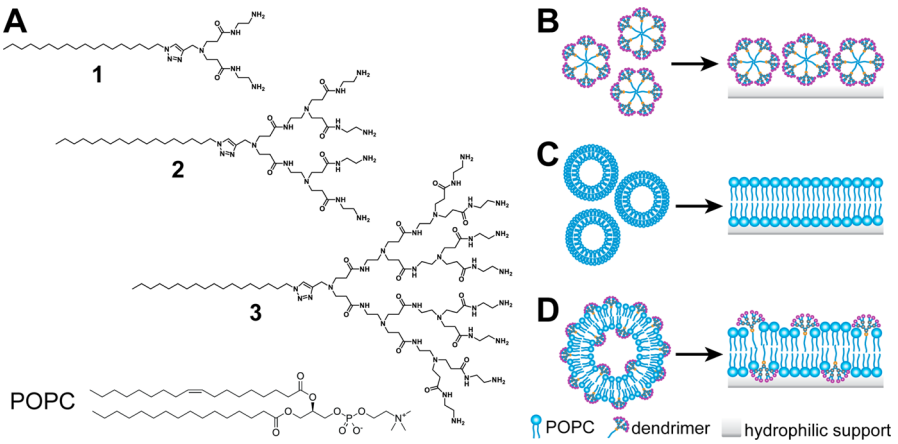

Figure 1. Molecular structures and supramolecular assembly pathways. (A) Molecular structures of amphiphilic dendrimers **1**−**3** and POPC used in this study. (B−D) Cartoon illustrations of (B) adsorption of amphiphilic dendrimer micelles onto a hydrophilic support, (C) fusion of phosphocholine vesicles on a hydrophilic support, and (D) fusion of hybrid POPC/dendrimer liposomes on a hydrophilic support.

investigated the coassembly processes of amphiphilic dendrimers **1**−**3** with palmitoyloleoylphosphocholine (POPC), a major component of the plasma membrane (Figure 1). We used surface plasmon resonance (SPR) spectroscopy to characterize the dendrimer and lipid coassembly processes on nanoglassified sensor chips[19,20] and performed confocal fluorescence microscopy studies to inspect the spatial organization of embedded and tagged components. Our results demonstrate that the amphiphilic dendrimers and POPC are capable of coassembling into uniform nanovesicles in solution, while also forming bilayer structures on hydrophilic glass supports. The hybrid membrane structures exhibit high lateral mobility—a trait common to natural lipid membranes—yet the bilayer stability and fluidity can be directly modulated by changing the dendrimer concentration and generation. In addition, *in situ* derivatization of the coassembled system can be achieved through nondestructive tagging of the dendrimer terminals with a protein-recognizing ligand, demonstrating the promise of the hybrid interface to function toward an enhanced supramolecular sensor and/or targeting device.

EXPERIMENTAL SECTION

Extended details regarding materials, preparatory techniques, and simulation protocols are provided in the Supporting Information. Amphiphilic dendrimers **1**, **2**, and **3** were synthesized according to previously reported methods (Scheme S1, Supporting Information).[10] The dendrimers were incorporated into standard sonication and extrusion techniques for hybrid dendrimer/POPC vesicle preparations. In brief, an appropriate amount of POPC and/or dendrimer stock solution in chloroform was dried in a glass vial under nitrogen to form a thin lipid film. The vial containing lipids was then placed in a vacuum desiccator for at least 2 h to remove any residual solvent. The dried lipids were resuspended in 1 × PBS to a lipid concentration of 1.0 mg/mL. After vigorous vortexing to remove all lipid remnants from the vial wall, the solution was bath sonicated for 30 min. Thereafter, the supernatant was extruded through a polycarbonate filter (Whatman, 100 nm) to produce small, unilamellar vesicles (SUVs) of uniform size. For fluorescence analysis, vesicle preparation followed the same procedure with the addition of 2% (w/w) NBD-PC, and dendrimer micelles were prepared with 1% (w/w) R18. All vesicle suspensions were used within 1 week and stored at 4 °C.

SPR spectroscopy and fluorescence microscopy were conducted on a NanoSPR5-321 (NanoSPR, Chicago, IL) and an inverted Leica TCS SP5 II (Leica Microsystems, Buffalo Point, IL), respectively, using previously established protocols for supported lipid bilayer analysis.[20] The SPR setup utilized a running buffer of 1 × PBS set to a flow rate of 5 mL/h (ca. 83 μL/min) unless otherwise noted.[21] The methods of Axelrod and Soumpasis were applied to fluorescence recovery after photobleaching (FRAP) data sets for determination of diffusion coefficients and mobile fractions.[22,23] For transmission electron microscopy (TEM) analysis, samples were applied directly to carbon-coated copper TEM grids, oven-dried, and stained with uranyl acetate prior to imaging with a JEOL 3010 microscope operating at 300 kV. The simulations are based on dissipative particle dynamics (DPD), a mesoscopic coarse-grained simulation method routinely employed for soft materials and biomembrane-containing system calculations.[24,25]

RESULTS AND DISCUSSION

Amphiphilic compounds form different and distinct geometric assemblies that depend on both the molecular structure and the hydrophobic/hydrophilic balance.[26] Phosphocholine (PC) is a linear amphiphile capable of forming bilayer liposomes which, when exposed to a hydrophilic support, will rupture and fuse into a planar supported lipid bilayer (SLB) exhibiting high lateral mobility of the embedded lipids.[27] In contrast, dendrimer **3** is a conical amphiphilic molecule which readily self-assembles into nanomicelles.[14] We therefore performed our initial assessments on the interaction of micelles consisting solely of **3** with a POPC bilayer formed on nanoglassified sensor chips using SPR. As illustrated in Figure 2A, the first increase in the SPR sensorgram is due to POPC adsorption and fusion into a SLB (**I** in Figure 2A). Addition of dendrimer **3** micelles results in a notable increase in resonance angle ($\Delta\theta_{min}$ = 0.10°, **III** and **IV** in Figure 2A), which then gradually decreases back to the baseline POPC value following the buffer rinse process (**V** in Figure 2A and Figure S1, Supporting Information). This is indicative of weak adsorption of dendrimer micelles onto the POPC membrane and in agreement with the established macropinocytotic pathway for the internalization of dendrimer nanomicelles; i.e., amphiphilic dendrimers do not directly fuse or strongly interact with the biomembrane but rather are internalized by energy-driven cellular processes, such as endocytosis.[11]

To further inspect the interaction of the dendrimer micelles with the POPC bilayer-covered glass support, we performed molecular simulations (see Supporting Information for computational methods).[11,12,14,28] According to these calculations, the spherical micelle generated upon self-assembly of dendrimer **3** is able to land softly on the bilayer surface

DOI: 10.1021/acsami.6b11556
ACS Appl. Mater. Interfaces XXXX, XXX, XXX−XXX

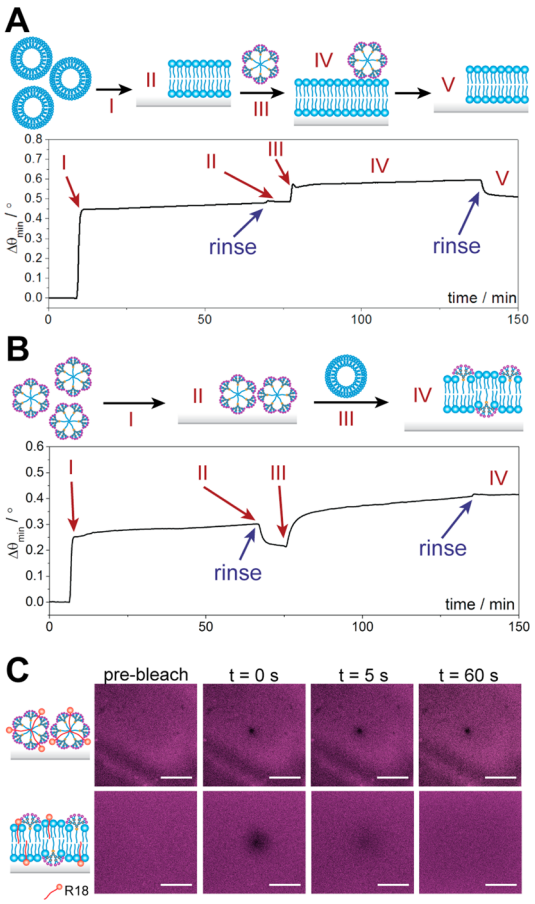

Figure 2. Coassembly interaction studies. (A, B) SPR studies on (A) fusion of POPC bilayers and transient adsorption of dendrimer **3** micelles and (B) adsorption of dendrimer **3** micelles and POPC-induced fusion. (C) FRAP studies on bleaching and recovery of dendrimer **3** micelles labeled with R18. Scale bars represent 30 μm.

whereupon it preserves its shape throughout the entire simulated process (10 μs) of its adhesion with the glass-supported POPC bilayer (see movie in Supporting Information). These results are in line with those obtained in SPR experiments, highlighting weak adsorption as opposed to irreversible fusion, of the dendrimer micelles to the POPC membrane.

Intriguingly, introducing dendrimer **3** to the silica-coated SPR chips results in a significantly smaller resonance angle change ($\Delta\theta_{min}$ = 0.20°, **I** in Figure 2B) compared to POPC ($\Delta\theta_{min}$ ~ 0.45°, **I** in Figure 2A). As SPR measures changes in the refractive index of the medium near the sensor interface,[29] the lower angular shift may be the result of intact micelle adsorption, leaving nanoscale buffer voids between adjacent structures which exhibit a lower net refractive index change. Confocal fluorescence microscopy was employed to investigate the adsorption of dendrimer micelles containing R18 onto the glass-supported POPC bilayer (Figure 2C, upper panel). R18 is a molecular probe with the fluorophore at the aqueous interface and the alkyl tail protruding into the lipid membrane interior, which when contained within dendrimer nanomicelles allows inspection of their spatial distribution. The images in Figure 2C (upper panel) reveal an even distribution of the micelles that are immobile, as shown by the lack of fluorescence redistribution after photobleaching, suggesting their intact adsorption onto the glass support.

To induce fusion of the dendrimer micellar structures with a model membrane and investigate the properties using surface-based analytical techniques, we next added POPC liposomes to obtain hybrid SLBs (**III** in Figure 2B) using established protocols.[30,31] Contrary to the previous experiment in which we added the dendrimer micelles to a preformed POPC membrane with which they interacted weakly (Figure 2A), here we incubated POPC vesicles with dendrimer micelles already adsorbed to the silica-coated surface (Figure 2B). Remarkably, the SPR sensorgram shows a net increase in the resonance angle after addition of the POPC vesicles (**III** in Figure 2B), which remains constant even after rinsing with buffer (**IV** in Figure 2B), resulting in a final $\Delta\theta_{min}$ of 0.41°. This finding suggests the incorporation of POPC into a hybrid lipid/dendrimer structure. We further studied this hybrid system using confocal fluorescence microscopy, which showed an even distribution of R18 with tagged PC. In this instance, however, fluorescence rapidly recovered after photobleaching, indicating a measurable lateral mobility in the membrane (lower panel in Figure 2C and Figure S2). To confirm that dendrimers were embedded in the POPC membrane and that we were not solely observing fusion of R18, we directly modified **2** with a fluorophore *in situ*, after fusion within the POPC bilayer, and also observed an even distribution of fluorescence (Figure S8). The long-range diffusion of both R18 and NBD-tagged phosphocholine (Figure S2) eliminates the possibility that the dendrimer micelles and phosphocholine vesicles remain adsorbed in their respective intact states and provides evidence for a coassembled lipid/dendrimer hybrid system with bilayer membrane fluidity.

Further investigations regarding the incorporation of amphiphilic dendrimers into fluid POPC bilayers required greater consistency among measurements as well as the ability to control the relative concentrations of dendrimers and POPC. Throughout the rest of the studies, we therefore mixed the POPC and dendrimers in varying ratios prior to liposome formation, using a previously developed protocol.[32] To inspect how the dendrimers and POPC coassemble in solution, we carried out dynamic light scattering (DLS) analysis and transmission electron microscopic (TEM) imaging on the mixed dendrimer/POPC assemblies. TEM imaging shows that the dendrimers alone form nanomicelles ca. 10 nm in diameter (Figure S3), in agreement with data previously established for **3** alone.[10] However, the hybrid dendrimer/POPC systems form larger, unilamellar vesicles (Figure 3A). Furthermore, DLS analysis revealed that the incorporation of dendrimers **1**−**3** into POPC liposomes did not notably affect their polydispersity but had a considerable impact on their size, with a decreasing average hydrodynamic vesicle diameter observed with higher generation dendrimers (Table S1). This decrease in size may be explained by considering the molecular geometry of POPC and dendrimers. POPC is a largely linear and cylindrical molecule, whereas dendrimers **1**−**3** are rather triangular and funnel-shaped. With increasing generation, the overall dendrimer shape becomes more conical, which likely produces some steric repulsion between the dendrimer terminals and adjacent POPC headgroups. Zeta potentials of the POPC vesicles were also affected by the dendrimers. Vesicles composed of POPC alone exhibited a near neutral zeta potential, whereas each of the hybrid lipid/dendrimer vesicle suspensions had a zeta potential of ca. +20 mV. This can be reasonably ascribed to the positively charged terminal amines that are present in each dendrimer in

DOI: 10.1021/acsami.6b11556
ACS Appl. Mater. Interfaces XXXX, XXX, XXX−XXX

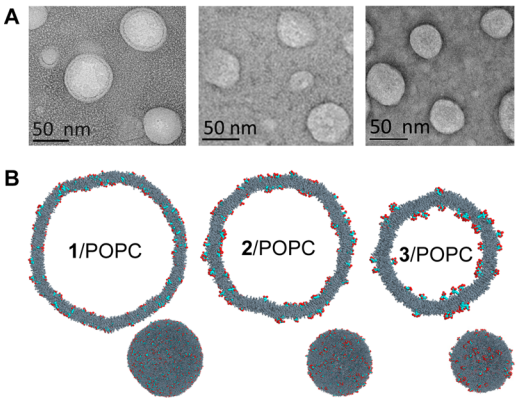

Figure 3. Coassembly structures. (A) TEM images and (B) simulated mesoscale morphologies of the mixed vesicles obtained from POPC and dendrimer **1** (left), **2** (center), and **3** (right). The POPC molecules are shown as dark gray spheres whereas the dendrimer molecules are highlighted in red for the hydrophilic part and blue for the hydrophobic part. Water molecules, ions, and counterions are not shown for clarity.

physiological buffer. Altogether, these data indicate that the dendrimers produce a fairly stable colloid with POPC.

In silico experiments further support these findings, with molecular simulations of mixed POPC/dendrimer systems yielding the stable unilamellar vesicles shown in Figure 3B. The calculated average dimensions of the vesicles and the corresponding zeta potential values (Table S2) are in agreement with the DLS data (Table S1). These snapshots extracted from the equilibrated simulation trajectories of the three mixed lipid/dendrimer vesicles revealed that dendrimers **1**, **2**, and **3** are all uniformly dispersed within the POPC bilayer, with no evidence of clustering or other structural organization. The hydrophobic portion of each dendrimer is inserted into the bilayer, while the charged heads are exposed on the surface of the corresponding self-assembled structures (Figure 3B). The enhanced conical shape and the high total charge (+8) of dendrimer **3** is reflected in a mixed vesicle configuration in which, by virtue of both steric and electrostatic repulsions with the POPC positive charges, the large branched charged head of **3** sticks out of the lipid bilayer and protrudes into the solvent somewhat more than the heads of the other two dendrimers. This allows for a tighter compaction of the bilayer and, consequently, for smaller vesicle dimensions. In summary, the overall uniform dispersion of dendrimers **1**, **2**, and **3** within the POPC bilayer ultimately generates mixed vesicles with optimal size and zeta potential to ensure that the most stable nanoparticles are formed in accordance with the corresponding situation.

Fusion of the hybrid dendrimer/POPC vesicles into an SLB was carried out following the same procedure as for traditional POPC vesicles; that is, the hybrid vesicles were applied to the surface of the glass support and incubated in an aqueous environment. The stability of these lipid bilayer structures upon introduction of a chemical perturbant was investigated using established SPR methods.[33] After vesicle fusion and rinsing of the membrane under PBS flowing at 5 mL/h, 0.1% (v/v) surfactant was introduced to the SPR flow cell at a rate of 20 mL/h, and buffer was rinsed through at this rate for 5 min. Upon return of the flow rate to 5 mL/h for 10 min, relative membrane removal was quantified through percent change of the minimum resonance angle as shown below, where $\Delta\theta_0$ represents the angular shift after vesicle fusion and $\Delta\theta_f$ represents the final angular shift after surfactant rinsing.

$$\text{membrane removal} = \frac{\Delta\theta_0}{\Delta\theta_f} \times 100\%$$

A representative sensorgram for these processes is shown in Figure 4A, which illustrates bilayer formation from the

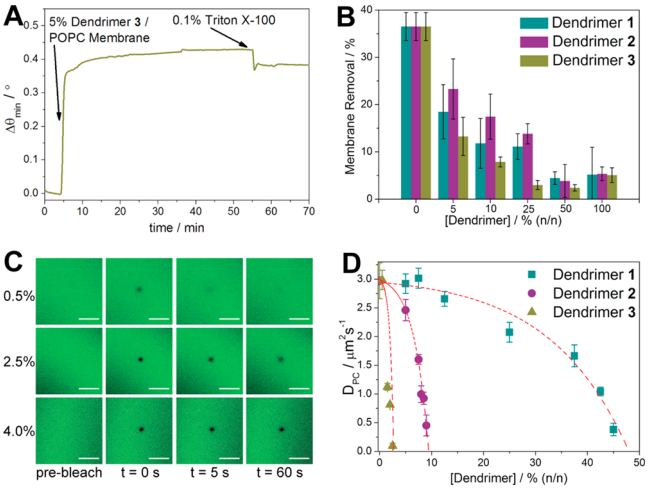

Figure 4. Biophysical studies of coassembled membranes. (A) Fusion of 5% **3**/POPC vesicles into support lipid bilayers (SLBs) followed by surfactant rinsing. (B) Percentage membrane removal based on dendrimer generation and concentration. (C) FRAP images of POPC membranes with increasing concentrations of **3**. Scale bars represent 30 μm. (D) Diffusion coefficients, indicative of POPC lateral mobility.

coassembled dendrimer/POPC vesicles, followed by the surfactant rinse. All three dendrimers appeared to have a concentration-dependent effect on the overall bilayer stability (Figure 4B). POPC alone exhibited the lowest stability (>35% membrane removal) in the presence of a relatively low concentration of surfactant. Increasing the concentration of dendrimers within the membrane imparted greater levels of stability (<10% membrane removal) up to a 50% (n/n)[34] composition of dendrimers and POPC.[35] The increased stability can be ascribed to the cooperative and multivalent interactions between the positively charged dendrimer amine terminals and the slightly negative glass support,[36] providing an *in situ* control of stability similar to previous findings with other fluidic membrane-embedded compounds.[37]

While the SPR stability studies provided us with an insight into the interactions between the hybrid coassemblies and their underlying supports, we further examined changes in POPC fluidity in response to dendrimer concentration and generation using fluorescence recovery after photobleaching (FRAP). We noted a decrease in the lateral mobility of fluorophore-labeled PC with increasing concentration of each dendrimer in the hybrid assemblies. This can be seen in the fluorescence images by the longer persistence of bleached areas with higher concentrations of the dendrimer (Figure 4C, also Figures S4–S6). Diffusion coefficients (D) for POPC show distinct patterns with increasing concentrations of **1**, **2**, and **3** (Figure 4D). Dendrimer **1** causes a gradual decrease in fluidity as its concentration within the membrane increases, eventually resulting in a loss of measurable fluidity above the levels of 45% (n/n) **1**. Dendrimer **2** follows a similar pattern, with a loss of fluidity above 8% (n/n) **2**, while **3** has the greatest impact,

DOI: 10.1021/acsami.6b11556
ACS Appl. Mater. Interfaces XXXX, XXX, XXX−XXX

causing a sharp decline in POPC mobility as soon as **3** is introduced. These results are intriguing because they show that each of the dendrimers has a direct, concentration-dependent impact on the surrounding lipid environment. The orientation of the zwitterionic headgroups of POPC (Figure 1A) within the bilayer leaves the positively charged ammonium groups positioned away from the bilayer/water interface and the negatively charged phosphates slightly buried. As increasing the dendrimer generation leads to more laterally extending terminal amines, the positively charged terminals can therefore be placed in an ideal position for attractive electrostatic forces with the POPC phosphate groups to take effect. This is corroborated by the bilayer reinforcement exhibited in the SPR assays. Taken together, our results demonstrate how the amphiphilic dendrimers enable fine-tuning of the biophysical properties of the hybrid bilayer interfaces.

Membranes composed of PC exhibit low biofouling and strong protein-resistant properties owing to their unique headgroup structures.[19,38] These are excellent characteristics for extending the detection limit in analytical sensors[19] and preventing degradation of liposomal therapeutics.[39] However, modifying the interfacial surface *in situ* currently presents a challenge in the development of new sensors and drug delivery tools. In our hybrid interfaces, the presence of the amine terminals on the embedded amphiphilic dendrimers enables the easy conjugation of biological recognition ligands, and we exemplify this by tagging of the hybrid dendrimer/lipid membranes with biotin, followed by streptavidin recognition. The SPR sensorgram shows formation of a hybrid **2**/POPC bilayer, followed by derivatization and protein recognition (Figure 5). We chose 5% (n/n) of **2** in the POPC bilayer

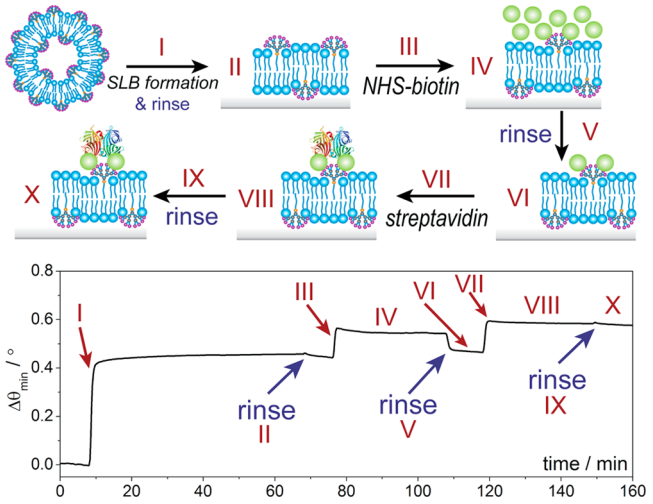

Figure 5. *In situ* derivatization of hybrid 5% **2**/POPC membranes with biotin, followed by streptavidin recognition.

membrane, as it offered a sufficient availability of free amine terminals for conjugation with biotin, yet a good balance of increased stability and retention of lateral lipid mobility. Following formation of the hybrid **2**/POPC bilayer (**I** and **II** in Figure 5), we added the NHS active form of biotin and incubated for 30 min. An increase in angular resonance ($\Delta\theta_{min}$ of 0.02°) was observed, indicating successful attachment of biotin to the free amine terminals (**III** and **IV** in Figure 5). After rinsing with PBS to remove unbound biotin (**V** and **VI** in Figure 5), we added streptavidin (1 μM), which resulted in a significant increase in angular resonance ($\Delta\theta_{min}$ = 0.11°) (**VII** and **VIII** in Figure 5). This can be ascribed to the recognition and binding of biotin/streptavidin, which remained constant even after copious rinsing with buffer (**X** in Figure 5). The interaction here is strong and specific for the dendrimer-containing membranes, in contrast with a control experiment in which an SLB composed of 100% POPC, where both NHS-biotin tagging and streptavidin recognition were unsuccessful (Figure S7). Verification of this process was also performed under fluorescence, in which a 5% **2**/POPC SLB on glass was exposed to an amine-reactive fluorophore (NHS-AMCA). Coupling of AMCA with the dendrimer containing membranes revealed an even distribution of AMCA fluorescence, with no observable damage to the membrane itself (Figure S8). The *in situ* derivatization exemplified here could be useful for developing high-performance sensors, as well as drug delivery carriers where the protein corona surrounding the complex can be dynamically altered without damaging the supramolecular architecture.[40,41]

CONCLUSIONS

In summary, the lipid/dendrimer coassembly processes investigated here have provided insights into the function and activity of the resulting biomimetic supramolecular complexes and interfaces. Separate constructions of amphiphilic dendrimer micelles and phosphocholine bilayers alone yielded few measurable interactions between the two systems, while coassembly of these materials into hybrid systems resulted in a new interface with tunable biophysical properties. Varying dendrimer generation and concentration allows modulating these hybrid interfaces with regards to stability, fluidity, and availability of derivatization sites and enables the creation of enhanced supramolecular entities with potentially interesting interfacial applications. This is the first study of amphiphilic dendrimers coassembled in a model membrane system. The potential directions to now be taken to gain further insight into additional assembly pathways and interfacial recognition schemes are multiple. Future studies will be geared toward accurately modulating and potentially controlling the behavior of this system toward tailored and specific applications.

ASSOCIATED CONTENT

Supporting Information

The Supporting Information is available free of charge on the ACS Publications website at DOI: 10.1021/acsami.6b11556.

Experimental details, Figures S1−S10, and Tables S1 and S2 (PDF)

Movie S1 (MPG)

AUTHOR INFORMATION

Corresponding Authors

*E-mail: quan.cheng@ucr.edu (Q.C.).

*E-mail: ling.peng@univ-amu.fr (L.P.).

ORCID

Samuel S. Hinman: 0000-0002-7727-0450

Erik Laurini: 0000-0001-6092-6532

Paola Posocco: 0000-0001-8129-1572

Sabrina Pricl: 0000-0001-8380-4474

Quan Cheng: 0000-0003-0934-358X

Notes

The authors declare no competing financial interest.

DOI: 10.1021/acsami.6b11556
ACS Appl. Mater. Interfaces XXXX, XXX, XXX−XXX

■ ACKNOWLEDGMENTS

We acknowledge support from the National Science Foundation (CHE-1413449 to Q.C.), Ligue Nationale Contre le Cancer (to L.P.), Association pour la Recherche sur les Tumeurs de la Prostate (to L.P.), and Agence National de la Recherche in the framework of EuroNanoMed II (to L.P.). S.S.H. was supported by a NIEHS T32 training grant (T32 ES018827) and Y.C. by Fondation de Recherche Médicale. We are grateful to Prof. Yadong Yin for the use of the particle analyzer. Fluorescence images were generated at the Microscopy Core/Center for Plant Cell Biology within the Institute for Integrative Genome Biology of the University of California, Riverside.

■ REFERENCES

(1) Lehn, J. M. Toward Self-Organization and Complex Matter. *Science* **2002**, *295*, 2400−2403.
(2) Aida, T.; Meijer, E. W.; Stupp, S. I. Functional Supramolecular Polymers. *Science* **2012**, *335*, 813−817.
(3) Webber, M. J.; Appel, E. A.; Meijer, E. W.; Langer, R. Supramolecular Biomaterials. *Nat. Mater.* **2015**, *15*, 13−26.
(4) Pamies, P.; Stoddart, A. Materials for Drug Delivery. *Nat. Mater.* **2013**, *12*, 957.
(5) Svenson, S. The Dendrimer Paradox–High Medical Expectations but Poor Clinical Translation. *Chem. Soc. Rev.* **2015**, *44*, 4131−4144.
(6) Mintzer, M. A.; Grinstaff, M. W. Biomedical Applications of Dendrimers: A Tutorial. *Chem. Soc. Rev.* **2011**, *40*, 173−190.
(7) Esfand, R.; Tomalia, D. A. Poly(Amidoamine) (PAMAM) Dendrimers: From Biomimicry to Drug Delivery and Biomedical Applications. *Drug Discovery Today* **2001**, *6*, 427−436.
(8) Tomalia, D. A.; Baker, H.; Dewald, J.; Hall, M.; Kallos, G.; Martin, S.; Roeck, J.; Ryder, J.; Smith, P. A New Class of Polymers - Starburst-Dendritic Macromolecules. *Polym. J.* **1985**, *17*, 117−132.
(9) Tomalia, D. A.; Naylor, A. M.; Goddard, W. A. Starburst Dendrimers - Molecular-Level Control of Size, Shape, Surface-Chemistry, Topology, and Flexibility from Atoms to Macroscopic Matter. *Angew. Chem., Int. Ed. Engl.* **1990**, *29*, 138−175.
(10) Yu, T. Z.; Liu, X. X.; Bolcato-Bellemin, A. L.; Wang, Y.; Liu, C.; Erbacher, P.; Qu, F. Q.; Rocchi, P.; Behr, J. P.; Peng, L. An Amphiphilic Dendrimer for Effective Delivery of Small Interfering RNA and Gene Silencing in Vitro and in Vivo. *Angew. Chem., Int. Ed.* **2012**, *51*, 8478−8484.
(11) Wei, T.; Chen, C.; Liu, J.; Liu, C.; Posocco, P.; Liu, X.; Cheng, Q.; Huo, S.; Liang, Z.; Fermeglia, M.; Pricl, S.; Liang, X. J.; Rocchi, P.; Peng, L. Anticancer Drug Nanomicelles Formed by Self-Assembling Amphiphilic Dendrimer to Combat Cancer Drug Resistance. *Proc. Natl. Acad. Sci. U. S. A.* **2015**, *112*, 2978−2983.
(12) Liu, X. X.; Zhou, J. H.; Yu, T. Z.; Chen, C.; Cheng, Q.; Sengupta, K.; Huang, Y. Y.; Li, H. T.; Liu, C.; Wang, Y.; Posocco, P.; Wang, M. H.; Cui, Q.; Giorgio, S.; Fermeglia, M.; Qu, F. Q.; Pricl, S.; Shi, Y. H.; Liang, Z. C.; Rocchi, P.; Rossi, J. J.; Peng, L. Adaptive Amphiphilic Dendrimer-Based Nanoassemblies as Robust and Versatile siRNA Delivery Systems. *Angew. Chem., Int. Ed.* **2014**, *53*, 11822−11827.
(13) Liu, X. X.; Liu, C.; Zhou, J. H.; Chen, C.; Qu, F. Q.; Rossi, J. J.; Rocchi, P.; Peng, L. Promoting siRNA Delivery Via Enhanced Cellular Uptake Using an Arginine-Decorated Amphiphilic Dendrimer. *Nanoscale* **2015**, *7*, 3867−3875.
(14) Chen, C.; Posocco, P.; Liu, X.; Cheng, Q.; Laurini, E.; Zhou, J. H.; Liu, C.; Wang, Y.; Tang, J.; Dal Col, V.; Yu, T. Z.; Giorgio, S.; Fermeglia, M.; Qu, F. Q.; Liang, Z.; Rossi, J. J.; Liu, M.; Rocchi, P.; Pricl, S.; Peng, L. Mastering Dendrimer Self-Assembly for Efficient siRNA Delivery: From Conceptual Design to in Vivo Efficient Gene Silencing. *Small* **2016**, *12*, 3667−3676.
(15) Ruysschaert, T.; Sonnen, A. F. P.; Haefele, T.; Meier, W.; Winterhalter, M.; Fournier, D. Hybrid Nanocapsules: Interactions of Aba Block Copolymers with Liposomes. *J. Am. Chem. Soc.* **2005**, *127*, 6242−6247.
(16) Le Meins, J. F.; Schatz, C.; Lecommandoux, S.; Sandre, O. Hybrid Polymer/Lipid Vesicles: State of the Art and Future Perspectives. *Mater. Today* **2013**, *16*, 397−402.
(17) Schulz, M.; Binder, W. H. Mixed Hybrid Lipid/Polymer Vesicles as a Novel Membrane Platform. *Macromol. Rapid Commun.* **2015**, *36*, 2031−2041.
(18) Xiao, Q.; Yadavalli, S. S.; Zhang, S.; Sherman, S. E.; Fiorin, E.; da Silva, L.; Wilson, D. A.; Hammer, D. A.; Andre, S.; Gabius, H. J.; Klein, M. L.; Goulian, M.; Percec, V. Bioactive Cell-Like Hybrids Coassembled from (Glyco)Dendrimersomes with Bacterial Membranes. *Proc. Natl. Acad. Sci. U. S. A.* **2016**, *113*, E1134−E1141.
(19) Phillips, K. S.; Han, J. H.; Martinez, M.; Wang, Z. Z.; Carter, D.; Cheng, Q. Nanoscale Glassification of Gold Substrates for Surface Plasmon Resonance Analysis of Protein Toxins with Supported Lipid Membranes. *Anal. Chem.* **2006**, *78*, 596−603.
(20) Hinman, S. S.; Ruiz, C. J.; Drakakaki, G.; Wilkop, T. E.; Cheng, Q. On-Demand Formation of Supported Lipid Membrane Arrays by Trehalose-Assisted Vesicle Delivery for SPR Imaging. *ACS Appl. Mater. Interfaces* **2015**, *7*, 17122−17130.
(21) The flow rate utilized here is higher than those conventionally seen in SPR analyses (e.g., 5−50 μL/min) in order to screen for analytes with high affinity attachments and minimize false positives resulting from insufficient rinsing.
(22) Axelrod, D.; Koppel, D. E.; Schlessinger, J.; Elson, E.; Webb, W. W. Mobility Measurement by Analysis of Fluorescence Photobleaching Recovery Kinetics. *Biophys. J.* **1976**, *16*, 1055−1069.
(23) Soumpasis, D. M. Theoretical-Analysis of Fluorescence Photobleaching Recovery Experiments. *Biophys. J.* **1983**, *41*, 95−97.
(24) Murtola, T.; Bunker, A.; Vattulainen, I.; Deserno, M.; Karttunen, M. Multiscale Modeling of Emergent Materials: Biological and Soft Matter. *Phys. Chem. Chem. Phys.* **2009**, *11*, 1869−1892.
(25) Shillcock, J. C. Spontaneous Vesicle Self-Assembly: A Mesoscopic View of Membrane Dynamics. *Langmuir* **2012**, *28*, 541−547.
(26) Lu, J. R.; Zhao, X. B.; Yaseen, M. Biomimetic Amphiphiles: Biosurfactants. *Curr. Opin. Colloid Interface Sci.* **2007**, *12*, 60−67.
(27) Castellana, E. T.; Cremer, P. S. Solid Supported Lipid Bilayers: From Biophysical Studies to Sensor Design. *Surf. Sci. Rep.* **2006**, *61*, 429−444.
(28) Welsh, D. J.; Posocco, P.; Pricl, S.; Smith, D. K. Self-Assembled Multivalent Rgd-Peptide Arrays - Morphological Control and Integrin Binding. *Org. Biomol. Chem.* **2013**, *11*, 3177−3186.
(29) Couture, M.; Zhao, S. S.; Masson, J. F. Modern Surface Plasmon Resonance for Bioanalytics and Biophysics. *Phys. Chem. Chem. Phys.* **2013**, *15*, 11190−11216.
(30) Dodd, C. E.; Johnson, B. R. G.; Jeuken, L. J. C.; Bugg, T. D. H.; Bushby, R. J.; Evans, S. D. Native E. Coli Inner Membrane Incorporation in Solid-Supported Lipid Bilayer Membranes. *Biointerphases* **2008**, *3*, FA59−FA67.
(31) Costello, D. A.; Hsia, C. Y.; Millet, J. K.; Porri, T.; Daniel, S. Membrane Fusion-Competent Virus-Like Proteoliposomes and Proteinaceous Supported Bilayers Made Directly from Cell Plasma Membranes. *Langmuir* **2013**, *29*, 6409−6419.
(32) Ghang, Y. J.; Lloyd, J. J.; Moehlig, M. P.; Arguelles, J. K.; Mettry, M.; Zhang, X.; Julian, R. R.; Cheng, Q.; Hooley, R. J. Labeled Protein Recognition at a Membrane Bilayer Interface by Embedded Synthetic Receptors. *Langmuir* **2014**, *30*, 10161−10166.
(33) Han, J. H.; Taylor, J. D.; Phillips, K. S.; Wang, X.; Feng, P.; Cheng, Q. Characterizing Stability Properties of Supported Bilayer Membranes on Nanoglassified Substrates Using Surface Plasmon Resonance. *Langmuir* **2008**, *24*, 8127−33.
(34) Composition in mole percent, here represented as n/n.
(35) Interestingly, there is a slightly higher amount of material removed when dendrimer micelles are applied alone, though this may be due to a lack of adsorbed supramolecular fusion. It should also be noted that higher concentrations of surfactant, ca. 1% or 5% Triton X-

DOI: 10.1021/acsami.6b11556
ACS Appl. Mater. Interfaces XXXX, XXX, XXX−XXX

552 100, resulted in near complete or complete removal of material for all
553 compositions.
554 (36) Behrens, S. H.; Grier, D. G. The Charge of Glass and Silica
555 Surfaces. *J. Chem. Phys.* **2001**, *115*, 6716−6721.
556 (37) Holden, M. A.; Jung, S. Y.; Yang, T. L.; Castellana, E. T.;
557 Cremer, P. S. Creating Fluid and Air-Stable Solid Supported Lipid
558 Bilayers. *J. Am. Chem. Soc.* **2004**, *126*, 6512−6513.
559 (38) Groves, J. T.; Mahal, L. K.; Bertozzi, C. R. Control of Cell
560 Adhesion and Growth with Micropatterned Supported Lipid
561 Membranes. *Langmuir* **2001**, *17*, 5129−5133.
562 (39) Farhood, H.; Serbina, N.; Huang, L. The Role of Dioleoyl
563 Phosphatidylethanolamine in Cationic Liposome Mediated Gene
564 Transfer. *Biochim. Biophys. Acta, Biomembr.* **1995**, *1235*, 289−295.
565 (40) Cedervall, T.; Lynch, I.; Foy, M.; Berggard, T.; Donnelly, S. C.;
566 Cagney, G.; Linse, S.; Dawson, K. A. Detailed Identification of Plasma
567 Proteins Adsorbed on Copolymer Nanoparticles. *Angew. Chem., Int.*
568 *Ed.* **2007**, *46*, 5754−5756.
569 (41) Lundqvist, M.; Stigler, J.; Elia, G.; Lynch, I.; Cedervall, T.;
570 Dawson, K. A. Nanoparticle Size and Surface Properties Determine the
571 Protein Corona with Possible Implications for Biological Impacts. *Proc.*
572 *Natl. Acad. Sci. U. S. A.* **2008**, *105*, 14265−14270.

DOI: 10.1021/acsami.6b11556
ACS Appl. Mater. Interfaces XXXX, XXX, XXX−XXX